The 8th TSME International Conference on Mechanical Engineering
12-15 December 2017
Bangkok, Thailand

AMM0019

Examination of cutting edge shape on multi-facet tool in ultra-precision cutting

Keisuke Amaki[1, *], Yukio Maeda[1], Kazuya Kato[2], Hideki Tanaka[2], Takanori Yazawa[3], and Tatsuki Otsubo[3]

[1] Toyama Prefectural University, 5180 Kurokawa, Imizu-shi, Toyama 939-0398, Japan
[2] Shonan Institute of Technology, 1-1-25 Tsujido-nishikaigan, Fujisawa-shi, Kanagawa 251-0046, Japan
[3] Nagasaki University, 1-14 Bunkyo-machi, Nagasaki-shi, Nagasaki 852-8521, Japan

*Corresponding Author: Keisuke Amaki:keisuke.amaki.29@gmail.com

Abstract. Recently, high efficiency and high performance have become requirements of equipment, such as laser printers. As a result, optical scanning parts that reduce optical aberration, scatter, and diffraction are required in laser printers. In the case of optical scanning parts, polygon mirrors are manufactured by polishing a plating or glassy material to a mirror finish. In this study, we shortened the manufacturing process to improve the production speed and ultra-precision cutting technology for polygon mirrors made of Al-Mg alloys. It is necessary to improve the geometric surface roughness achieved in mirror cutting of Al-Mg alloys and to remove tear-out marks and scratch marks that occur during the cutting process. We investigated the cutting edge shape using a straight diamond tool to decrease the surface defects during ultra-precision cutting of Al-Mg alloys. We chose two characteristic triple-facet tools, denoted (A) and (B), and investigated the cutting edge shape using these tools. We found that the triple-facet diamond tool (B) could achieve a good machined surface without surface defects. Therefore, we produced three quattro-facet tools to evaluate the cutting edge of the triple-facet tool (B). We investigated the influence of the cutting edge of each tool on the surface defects in the ultra-precision cutting of Al-Mg alloys.

1. Introduction

Recently, high efficiency and high performance have become essential requirements of equipment such as laser printers [1, 2]. As a result, optical scanning parts that reduce optical aberration, scatter, and diffraction in laser printers are in considerable demand [3, 4]. Figure 1 shows examples of microphotographs and surface roughness profiles of machined surfaces [5]. In this study, we shortened the manufacturing process to improve the production speed and ultra-precision cutting technology for polygon mirrors made of aluminum alloys. It is necessary to improve the geometric surface roughness achieved during the mirror cutting of Al-Mg alloys and to remove the tear-out marks and scratch marks that occur during the cutting process. Therefore, we investigated the shape of the cutting edge using a diamond tool to reduce surface defects during the ultra-precision cutting of Al-Mg alloys.

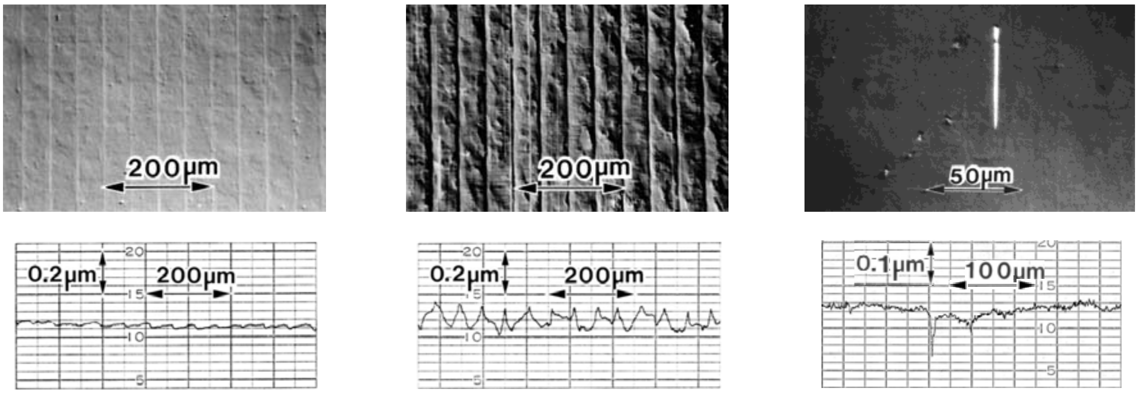

(a) Feed marks. (b) Tear-out marks. (c) Scratch marks.

Figure 1. Photographs and surface roughness profiles of machined surfaces.

2. Experiment equipment and configuration

The cutting conditions are summarized in Table 1, and the experimental setup is shown in figure 2. Machined surface damage due to entwining chips was controlled using the minimum quantity of lubrication (MQL) required and a chip collector.

Table 1. Experimental equipment and conditions.

Machine tool	NC ultra-precision turning machine ULG100C
Cutting tool	Diamond tool (single crystal diamond)
Work piece	A5186 OD 130mm× ID 40mm
Cutting conditions	Cutting speed : V=193～628 m/min Feed rate : F=50 ~ 200 μm/rev Depth of cut : t =30 μm Tool setting angle θ : 0° ~ 0.05°
Lubricating system	MQL
Cutting fluid	UP-2A
Chip collector	GSB-10537exP
Dynamometer	Type9251A KISTLER

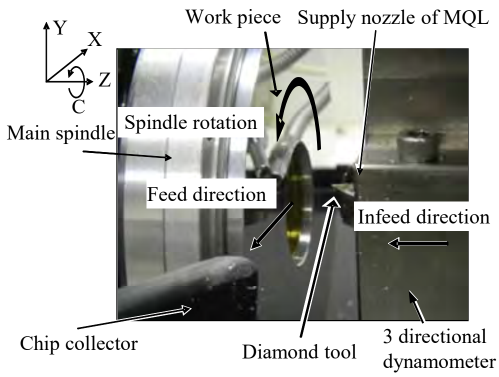

Figure 2. Setup of experiment.

3. Results from prior experimentation

3.1. Straight tool and double-facet tool

When using a straight tool with a positive tool setting angle, the surface roughness increases, because tear-out marks occur on the side cutting edge. With a negative tool setting angle, we achieved a good machined surface without tear-out marks. The reason for this is that the tear-out marks were removed by the end cutting edge. However, these methods cannot support a high feed rate, since it is a time-consuming process. A straight tool was used to produce a good machined surface without tear-out marks for a narrow range of tool setting angles θ from −0.015° to −0.008° [9-11]. We produced a double-facet tool to expand this tool setting angle range. In addition, it was difficult to give a direct micro-facet. Therefore, we developed a double-facet tool with a side rake angle on the rake face to produce a pseudo-facet. The use of the double-facet tool resulted in a 10-fold increase in the range of the tool setting angle. This produced a good machined surface without tear-out marks. However, there were scratch marks on the machined surface from using a straight tool and a double-facet tool [12]. Therefore, we investigated the mechanism of scratch marks.

3.2. *Mechanism of scratch formation*

The mechanism of scratch formation is shown in figure 3. We found that the tool crashed against bumps formed by crystallization producing small pieces. Then, these pieces would attach to the end of the cutting edge and act as micro cutting edges. As a result, these small pieces caused the scratch marks. Therefore, we expect that the ductility-mode processing of an inclusion is possible if the depth of the cut is small. Based on the mechanism of scratch mark generation, ductility-mode processing of an inclusion can be expected if the depth of the cut is small. We developed a triple-facet tool with a double-facet at the end cutting edge to remove scratch marks and investigated its influence on surface defects.

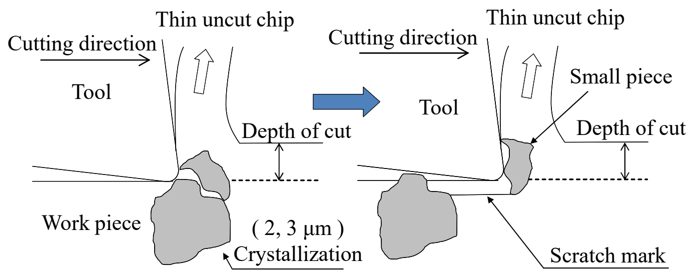

Figure 3. Schematic of scratch mark formation tool.

3.3. *Triple-facet tool*

Figure 4 shows the cutting edge shape of the triple facet tool. The triple-facet tool has two micro-facets at the end cutting edge and can perform micro-cuts. Additionally, for the triple-facet tool, the micro-facet β_2 removes tear-out marks, and micro-facet β_1 removes scratch marks. The removal of tear-out marks and scratch marks separately by each micro-facet produces a good machined surface. We developed four triple-facet tools and selected two triple-facet tools, which were denoted as triple-facet tool (A) and triple-facet tool (B). Figure 5 shows enlarged views of the end cutting edges of triple-facet tools (A) and (B). In triple-facet tool (A), the measured cutting edge shape has an ideal cutting edge shape. In triple-facet tool (B), there was a curved portion on the end cutting edge and micro-facet β_1. This curved portion is marked as a red line. We investigated the influence of surface defects using triple-facet tools (A) and (B). As a result, for an in feed rate of F=200 μm/rev, the use of triple-facet tools (A) and (B) both resulted in a good machined surface roughness with a tool setting angle in the range of 0° to 0.04°. Next, we investigated the relationship between scratch marks and the undeformed chip thickness.

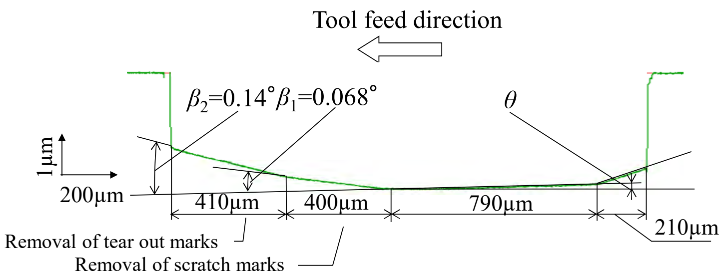

Figure 4. Cutting edge shape of triple-facet tool.

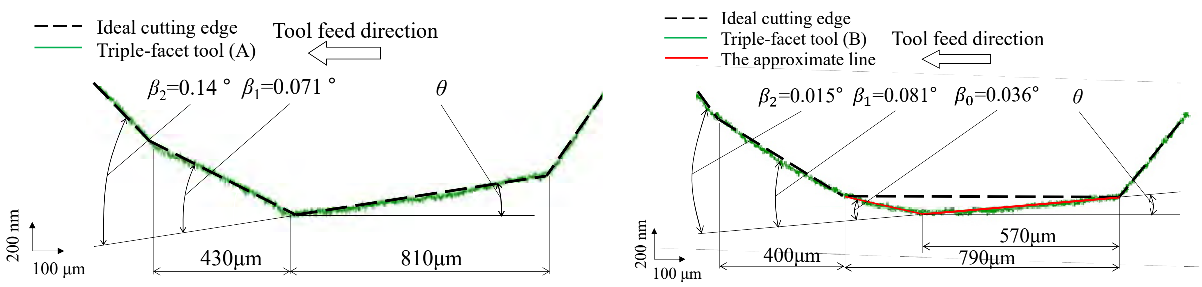

(a) Triple-facet tool (A). (b) Triple-facet tool (B).

Figure 5. Enlarged view of cutting edge shape of triple-facet tools.

Figure 6 shows relationships between the tool setting angle θ and the undeformed chip thickness n with triple-facet tool (A) and (B). The undeformed chip thickness n is calculated by equations (1) and (2). In these equations, "F" is feed rate, "β" is micro-facet angle. In equation (1), tool setting angle ranges is from 0° to 0.071° with triple-facet tools (A). In equation (2), tool setting angle ranges is from 0° to 0.036° with triple-facet tool (B). Based on these results, we found that using the triple-facet diamond tool (B) with a curved portion on the end cutting edge could achieve a good machined surface without surface defects when the undeformed chip thickness is less than 100 nm. Therefore, we produced three quattro-facet tools to evaluate cutting edge of the triple-facet tool (B). We investigated the influence of the cutting edge of each of the tools on the surface defects in the ultra-precision cutting of Al-Mg alloys.

$$n = F \times \sin(\beta_1 - \theta) \tag{1}$$

$$n = F \times \sin(\beta_0 - \theta) \tag{2}$$

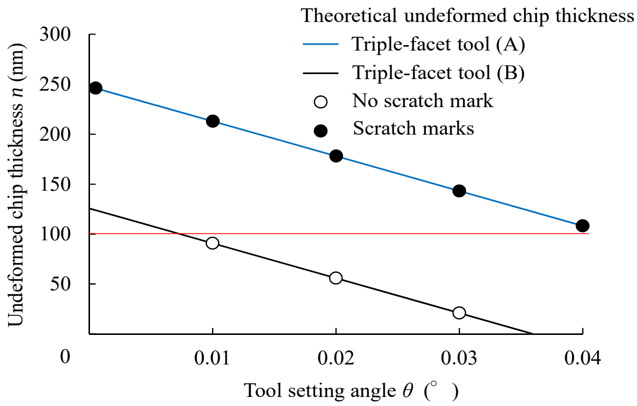

Figure 6. Relationships between tool setting angle θ and undeformed chip thickness n with triple-facet tool (A) and (B).

4. Cutting characteristics of quattro-facet tools

Figure 7 shows the cutting edge shapes of the quattro-facet tools (C), (D), and (E). In quattro-facet tools (C), (D), and (E), we assumed a micro cutting edge angle β_0 nearly fixed and varied the micro cutting edge angle β_1 from 0.033° to 0.077°. The cutting edge shape of quattro-facet tool (C) is like the triple-facet tool (B). We changed the micro cutting edge angle β_1 to 0.051° in quattro-facet tool (D) and changed the micro cutting edge angle β_1 to 0.033° in the quattro-facet tool (E). Using these quattro-facet tools, we investigated the influence of surface defects.

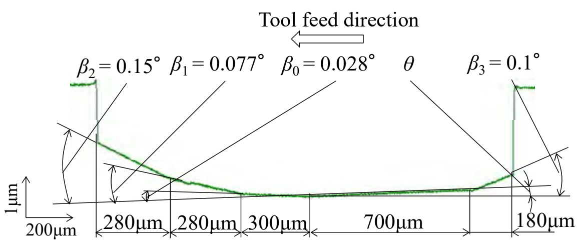

(a) Quattro-facet tool (C).

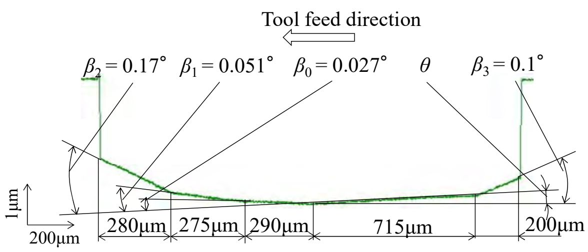

(b) Qattro-facet tool (D).

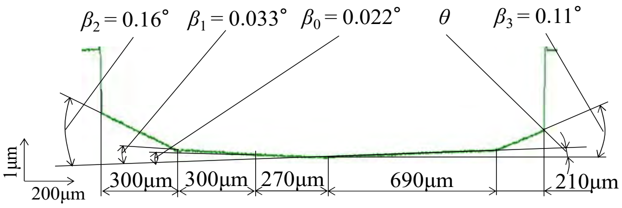

(c) Quattro-facet tool (E).

Figure 7. Cutting edge shape of triple-facet tools.

Figure 8 shows the relationship between the tool setting angle θ and the surface roughness Rz at a tool feed rate of 200 μm/rev with quattro-facet tools (C), (D) and (E). The theoretical surface roughness Hth is calculated by equations (3), (4), and (5). In equation (3), tool setting angle ranges is from 0° to 0.028° in quattro-facet tool (C), from 0° to 0.027° in quattro-facet tool (D), and from 0° to 0.022° in quattro-facet tool (E). In equation (4), tool setting angle ranges is from 0.028° to 0.077° in quattro-facet tool (C), from 0.027° to 0.055° in quattro-facet tool (D), and from 0.022° to 0.033° in quattro-facet tool (E). In equation (5), tool setting angle range is from 0.033° to 0.16° in quattro-facet tool (E). The use of quattro-facet tools (C) and (D) achieved a good machined surface roughness with a tool setting angle in the range of 0° to 0.05°. Using quattro-facet tool (E), we achieved a good machined surface roughness with a tool setting angle in the range of 0° to 0.03°. However, in the range of 0.04° to 0.05°, we could not achieve a surface roughness Rz less than 40 nm. For the cause of this, it is thought that micro tear-out marks occurred on the machined surface. Next, we investigated the relationship between the scratch marks and the undeformed chip thickness.

$$\mathrm{Hth} = \frac{f}{\cot\theta + \cot(\beta_0 - \theta)} \tag{3}$$

$$\mathrm{Hth} = \frac{f}{\cot(\beta_1 - \theta) + \cot(\theta - \beta_0)} \tag{4}$$

$$\mathrm{Hth} = \frac{f}{\cot(\beta_2 - \theta) + \cot(\theta - \beta_1)} \tag{5}$$

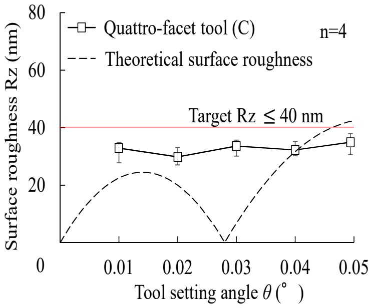

(a) Quattro-facet tool (C).

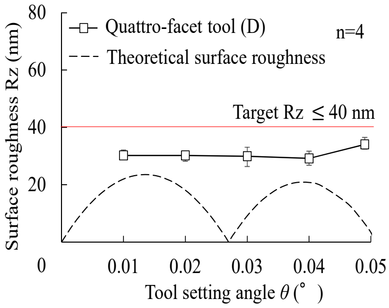

(b) Quattro-facet tool (D).

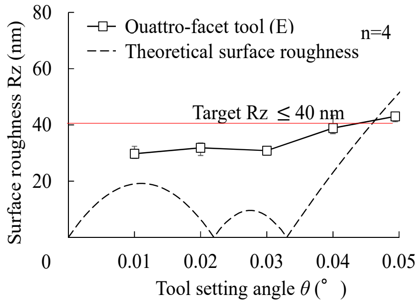

(c) Quattro-facet tool (E).

Figure 8. Relationship between tool setting angle θ and the surface roughness Rz.

Figure 9 shows the relationships between the tool setting angle and undeformed chip thickness with quattro-facet tools (C), (D), and (E). The undeformed chip thickness n is calculated by equations (6) and (7). In equation (6), tool setting angle ranges are from 0° to 0.028° in quattro-facet tool (C), from 0° to 0.027° in quattro-facet tool (D), and from 0° to 0.022° in quattro-facet tool (E). In equation (7), tool setting angle ranges are from 0.027° to 0.077° in quattro-facet tool (C), from 0.027° to 0.051° in quattro-facet tool (D), and from 0.022° to 0.033° in quattro-facet tool (E). These results indicate that when using quattro-facet tool (C) there were scratch marks on the machined surface for a tool setting angle in the range of 0.03° to 0.05°. Using quattro-facet tools (D) and (E) could decrease the scratch marks using a tool setting angle in the range of 0° to 0.05° when the chip thickness was less than 100 nm. Also, The use of the quattro-facet tool results in a 1.5 times increase in the tool setting angle range able to reduce the scratch marks when the micro cutting edge angle β_1 is two times the micro cutting edge angle β_0.

$$n = F \times \sin(\beta_0 - \theta) \tag{6}$$
$$n = F \times \sin(\beta_1 - \theta) \tag{7}$$

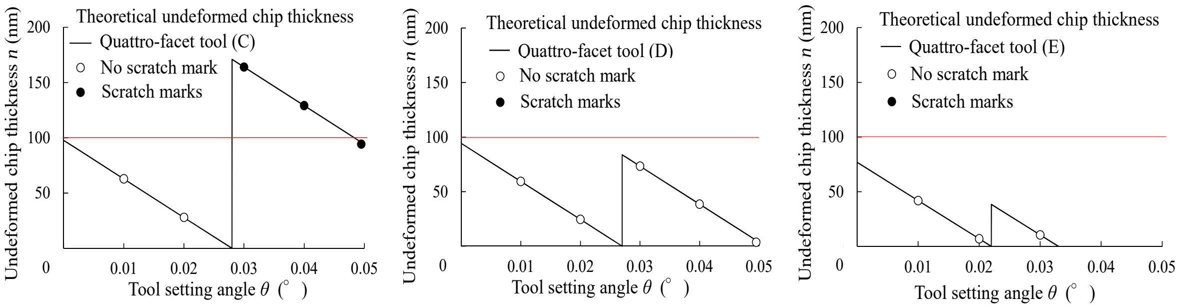

(a) Quattro-facet tool (C). (b) Quattro-facet tool (D). (c) Quattro-facet tool (E).

Figure 9. Relationship between tool setting angle and undeformed chip thickness.

Also, it was confirmed that there is ductility-mode cutting when the undeformed chip thickness is smaller than the radius of the tool's cutting edge [13-15]. Therefore, we measured the cutting edge radius of the quattro-facet tools. Figure 10 shows the cutting edge radius of the quattro-facet tool (C). We measured the radii using a Scanning Electron Microscope (SEM) of ELIONIX.

The results showed that the radii of the cutting edges for the quattro-facet tools (C), (D) and (E) were 108 nm, 120 nm, and 115 nm, respectively. The cutting edge radius of the quattro-facet tools (C), (D) and, (E) are larger than the undeformed chip thickness. Therefore, it is assumed that the use of the quattro-facet tools (C), (D) and, (E) achieved a machined surface without scratch marks when the undeformed chip thickness is less than 100 nm.

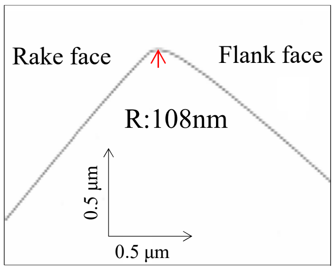

Figure 10. The tool cutting edge radius quattro-facet tool (C).

5. Conclusion

This study investigated the influence of undeformed chip thickness on scratch marks with quattro-facet tools. The following results were obtained.

(1) It is assumed that the use of the quattro-facet tools achieved a machined surface without scratch marks when the undeformed chip thickness is less than 100 nm which is smaller than the cutting edge radius of the quattro-facet tools.

(2) The use of quattro-facet tool results in a 1.5 times increase in the tool setting angle range able to reduce the scratch marks when the micro cutting edge angle β_1 is two times the micro cutting edge angle β_0.

References

[1] Kawamura A, Suzuki S and Hayashi Y 2003 *Hand of Laser Technology and Applications* (CRC press) pp 2421- 2462

[2] Matsuda T, Mikami T and Abe F 1983 *Journal of the Institute of Electronics, Information and Communication Engineers* **J6−C**(2) pp 137−144

[3] Kato Y, Umeda H and Hoshino K 2005 *Aluminum ally substrate for high density magnetic memory disks Kobe steel engineering reports* **55**(2)
[4] Whiteen L G and Lewis T G 1983 *Proc. M.T.D.R* p 491
[5] Maeda Y, Masami M, Nishiguchi T, Sawa M and Ito R 1986 *A Study on Diamond Turning of Al−Mg Alloy Generation Mechanism of Surface Machined with Worn Tool Annals of the CIRP* **38-1** pp 111-114
[6] Teaching materials development committee 1991 *Ultra-precision cutting of the polygon mirror Magazine of occupation development report* pp 9-10 (in Japanese)
[7] Tanaka K 1987 *Journal of Japan society for precision engineering* **53**(6) pp 23-24
[8] Ou H, Maeda Y, Sinji Y, Nisiguchi T and Masuda M *2000 Reduction of tear-out marks in diamond cutting of aluminum alloys High processing* **19** pp 42-48
[9] Maeda Y 1991 *Study on processing precision improvement in ultra-precision cutting Doctoral dissertation* pp 27-29
[10] Sawa M, Maeda Y and Masami M 1993 *Development of an advanced tool-setting device for diamond turning annals of the CIRP* **42** pp 87-90
[11] Iida T, Maeda Y, Hirase D, Motoyoshi T, Tanaka T, Kato K and Yazawa T 2015 *Advanced Materials Research* **806** pp 178-183
[12] Hirase D, Maeda Y, Iwatsuka K, Kato K and Yazawa T 2012 *Renewable Energy Research and Applications* (ICRERA) *Nov*. pp 1-6
[13] P.Li X, He T, Rahman M 2005 *Tool Wear Characteristics and Their Effects on Nanoscale Ductile Mode cutting of Silicon Wafer* **259** pp 1207-1214
[14] Cai M.B, Li X.P, Rahman M, Tay A.A.O 2007 *Crack initiation in Relation to the Tool Edge Radius and Cutting Conditions in Nanoscale Cutting of Silicon* **47** pp 562-569
[15] Cai M.B, Li X.P, Rahman M 2007 *Study of the Mechanism of Nanoscale Ductile Mode Cutting of Silicon Using Molecular Dynamics Simulation* **47** pp 75-80